Published in final edited form as:
Hear Res. 2013 June ; 300: 1–9. doi:10.1016/j.heares.2013.02.009.

A null mutation of mouse *Kcna10* causes significant vestibular and mild hearing dysfunction

Sue I. Lee[a], **Travis Conrad**[a,b], **Sherri M. Jones**[c], **Ayala Lagziel**[a], **Matthew F. Starost**[d], **Inna A. Belyantseva**[a], **Thomas B. Friedman**[a], and **Robert J. Morell**[a,*]

[a]Section on Human Genetics, Laboratory of Molecular Genetics, National Institute on Deafness and Other Communication Disorders, National Institutes of Health, Rockville, Maryland, USA

[b]Department of Hearing and Speech Sciences, University of Maryland, College Park, Maryland, USA

[c]Special Education and Communication Disorders, University of Nebraska-Lincoln, Lincoln, Nebraska, USA

[d]Office of Research Services in the Division of Veterinary Resources, NIH

Abstract

KCNA10 is a voltage gated potassium channel that is expressed in the inner ear. The localization and function of KCNA10 was studied in a mutant mouse, B6-*Kcna10*^{TM45}, in which the single protein coding exon of *Kcna10* was replaced with a beta-galactosidase reporter cassette. Under the regulatory control of the endogenous *Kcna10* promoter and enhancers, beta-galactosidase was expressed in hair cells of the vestibular organs and the organ of Corti. KCNA10 expression develops in opposite tonotopic gradients in the inner and outer hair cells. *Kcna10*^{TM45} homozygotes display only a mild elevation in pure tone hearing thresholds as measured by auditory brainstem response (ABR), while heterozygotes are normal. However, *Kcna10*^{TM45} homozygotes have absent vestibular evoked potentials (VsEPs) or elevated VsEP thresholds with prolonged peak latencies, indicating significant vestibular dysfunction despite the lack of any overt imbalance behaviors. Our results suggest that *Kcna10* is expressed primarily in hair cells of the inner ear, with little evidence of expression in other organs. The *Kcna10*^{TM45} targeted allele may be a model of human nonsyndromic vestibulopathy.

Keywords

KCNA10; inner ear; vestibular dysfunction; *Kcna10* knockout mouse

Corresponding author: Robert J. Morell, 5 Research Ct, 2A-19, Rockville, MD 20850, Telephone: 301-402-4249, morellr@nidcd.nih.gov.

SIL, AL and IAB designed and performed immunohistochemisty and beta-galactosidase expression studies and analyzed the results.

SMJ performed vestibular function experiments and analyzed VsEP data. MFS performed phenotype analysis of the B6-*Kcna10*^{TM45} strain. TC and RJM performed audiological experiments. RJM performed RT-PCR experiments and analyzed audiological data. SIL, IAB, TBF and RJM co-wrote the paper.

1. Introduction

There are twelve classes of mammalian voltage gated potassium channels classified according to the sequence similarity of their alpha subunits (Gutman et al, 2005). KCNA proteins, one class of voltage gated potassium channels, are encoded by the subfamily of *shaker* genes (*Kv1*), named for their homology to the *Shaker* potassium channel gene in *Drosophila* (Pongs, 1992). Mutations of the genes encoding the KCNA channels are implicated in human epilepsy (MIM 176260; Smart et al 1998) and episodic ataxia (MIM 160120; Browne et al 1994), and autoantibodies to KCNA channels (KCNA1, KCNA2, and KCNA6) are associated with acquired neuromyotonia (Kleopa et al 2006). KCNA channels have also been shown to play roles in binaural coincidence detection (Mathews et al, 2010) and the maturation of primary vestibular neurons (Iwasaki et al, 2012) although, due to the nature of these studies, it is challenging to determine which KCNAs were involved. Additionally, KCNAs have been found in the ventral cochlear nucleus (Wang et al, 1994), vestibular ganglion cells (Iwasaki et al, 2008), and the medial superior olive nucleus of the mammalian brain (Mathews et al, 2010).

KCNA10 shares 50 to 70% amino acid sequence identity with other KCNA protein family members, and is suspected to have a similar secondary structure to all KCNA channels (Tian et al, 2002). KCNA10 is unique among the KCNA family due to its putative cyclic nucleotide-binding domain at the carboxyl terminus (Yao et al, 1995), suggesting that KCNA10 may have features associated with both potassium voltage gated channels and nonselective cation channels (Lang et al, 2000). KCNA10 has been localized to rat glomerular endothelium and renal proximal tubule by immunohistochemistry, where it is hypothesized to play a role in stabilizing cell membrane voltage (Yao et al, 2002). Recently, KCNA10 was localized to the mouse organ of Corti and vestibular end-organs by immunohistochemistry (Carlisle et al 2012). Inspection of *Kcna10* signature sequences in more than 90 tissue-specific Massively Parallel Signature Sequencing (MPSS) cDNA libraries (Peters et al, 2007) indicates selective, almost exclusive, expression of this gene in the inner ear.

To determine the localization, developmental expression profile, and function of KCNA10 in the mouse inner ear, we evaluated a *Kcna10* knockout mouse (B6;-$Kcna10^{TM45}$). *Kcna10* is expressed primarily in the hair cells of both organ of Corti and vestibular sensory epithelia. The homozygous *Kcna10* knockout mouse ($Kcna10^{TM45/TM45}$) displayed a slightly elevated hearing threshold at higher frequencies and vestibular dysfunction.

2. Materials and Methods

2.1 RT-PCR

Kcna10 was amplified from mouse cDNA tissue panels MTC I and III (Clontech) and cDNA also synthesized from polyA RNA isolated from adult cochleae using Superscript RT (Invitrogen) using primers (5′-GAGACCAGCACATCCCATCT-3′) and (5′-TAGCCTGGCTCTTCATGGAT-3′). These primers are located in exons 1 and 3 and will generate a 479-bp amplimer from transcripts using cassette exon 2, and a 224-bp amplimer from transcripts without exon 2.

2.2 *Kcna10*–null mouse development

Mice segregating a knockout allele of *Kcna10* ($Kcna10^{TM45}$) on a C57Bl/6; 129SvEv mixed background were obtained from the Texas A&M Institute for Genomic Medicine. Exon 3 of *Kcna10* was replaced with an IRES-bGeo/Puro cassette; thus, the complete protein coding sequence of *Kcna10* was deleted. Details of the targeting construct and confirmation of homologous recombination in ES cells are shown in Supplementary Figure 1. The colony

was maintained by heterozygous x heterozygous crosses and all data reported herein were obtained from littermates.

The *Kcna10*^{TM45} allele was genotyped using two sets of primers. Due to the large size of the reporter and selection cassette, primer pairs were developed to amplify either the wild type or the mutant allele at each targeting construct insertion site. At the 5′ prime integration site, set A (common forward primer 5′-AGGGAATGATTGCTGCTGGA-3′, wild type reverse primer 5′-AAGGCAGTTTCATGGTTGGTG-3′, and mutant reverse primer 5′-AAGGCAGTTTCATGGTTGGTG-3′) amplifies fragments of 395 bp from the wild type allele and 530 bp from the mutant allele. At the 3′ integration site, set B (wild type forward primer 5′-GTGAGGGTCTTCCGCATCT-3′, wild type reverse primer 5′-GCCTCTTGGCCATAGAACAT-3′, mutant forward primer 5′-ATTGCATCGCATTGTCTGAG-3′, and mutant reverse primer 5′-AAGGCAGTTTCATGGTTGGTG-3′) amplifies fragments of 589 bp from the wild type allele and 530 bp from the mutant allele.

2.3 Detection of beta-galactosidase activity

Wild type and homozygous mutant *Kcna10*^{TM45} mice from embryonic day 18 (E18.5) to postnatal day 75 (P75) were sacrificed, and the embryo, brain, heart, lung, liver, kidney, and/or cochlea were harvested according to NIDCD/NIH animal protocol 1263-09. All organs except the cochlea and embryos were then dissected into similar sizes for uniform staining. All of the following solutions were made in PBS. Organs obtained for X-gal staining were fixed in a solution containing 2% paraformaldehyde, 2% glutaraldehyde, and 0.5% NP-40. Tissues were then washed twice for 30 minutes each with a buffer consisting of 0.5% NP-40 and 1mM $MgCl_2$ and stained overnight at 37°C with a solution containing 2.5 mM$K_3Fe(CN)_6$, 2.5 mM $K_4Fe(CN)_6$, 1 mM $MgCl_2$, and X-gal (40mg/mL, Sigma Aldrich B4252-1G). Cochleae older than P30 were then further incubated for 5 days in 250 mM EDTA and 2% paraformaldehyde. All tissues were then washed with PBS. Cochleae were further microdissected to extract sensory epithelia from the organ of Corti and vestibular organs. Tissues were imaged with a Zeiss StemiSV11 dissection microscope equipped with a Zeiss AxioCam camera and Axio Vision imaging software (Zeiss MicroImaging, Inc), or mounted on glass slides using Immu-Mount (Thermo Scientific) and imaged with a Zeiss LSM780 confocal microscope.

2.4 Auditory Brainstem Response (ABR)

Pure-tone stimuli were generated with the SmartEP (Intelligent Hearing Systems (IHS)) software and presented through a high-frequency transducer. ABR waveforms were elicited using rarefaction polarity tone bursts of 8, 16, 24, and 32 kHz at a rate of 21.1 per second. Tone burst stimuli were 3 ms in duration and shaped using a Blackman envelope.

Mice were handled according to the NIH animal care and use guidelines under NIDCD animal protocol #1263-09. ABR testing was performed at approximately 3 months age on five wild type, 15 heterozygous and 10 homozygous littermates. Mice were anesthetized with an intraperitoneal injection of a combination of 56mg/kg body weight of ketamine (Vedco) and 0.375mg/kg body weight of dexdomitor (Pfizer). Mice were maintained at 37°C during testing in a sound-proof booth (Acoustic Systems). To record auditory brainstem potentials, sterile subdermal needle electrodes were used, with one applied to the forehead, and one each behind the left and right pinnae. The right ear only was tested for each animal.

The stimulus intensity began at 100 dB SPL and was decreased in 10-dB steps until no ABR waveform could be seen. The procedure was repeated with 5-dB step decreases as threshold

was approached, until the lowest level replicable response was obtained, which was then considered to be threshold. After all threshold data were obtained for each tone burst stimulus, mice were administered a 0.01 ml/gram body weight dose of antisedan (Pfizer) and placed in a heated recovery cage. Waveforms elicited by 16-kHz stimuli at 90 dB SPL were used to determine absolute and interpeak latencies. Thresholds were compared using 2-way ANOVA unweighted means analysis with within-frequency post-test comparisons to heterozygote means corrected for multiple testing.

2.5 VsEP testing

Vestibular evoked potentials (VsEPs) were recorded for P30 (n = 9 heterozygotes, n = 6 homozygotes) and 10 month-old (n = 6 heterozygotes, n = 8 homozygotes) *Kcna10* knockout mice using methods published previously (Jones et al., 2011). Vestibular functional studies were completed at East Carolina University according to institutional animal use protocol #P026. Briefly, mice were anesthetized with a mixture of ketamine (90 – 126 mg/kg) and xylazine (10 – 14 mg/kg). Core body temperature was maintained at 37.0 ± 0.2°C. Electrodes were placed subcutaneously at the nuchal crest (non-inverting), behind the right pinna (inverting), and at the hip (ground). Tucker Davis Technology modules and custom software were used to present stimuli and record responses. Linear acceleration ramps (17 pulses/s, 2-ms duration) were presented to the cranium in the naso-occipital axis. A noninvasive head clip was used to secure the head to a mechanical shaker for delivery of vestibular stimuli. Stimulus levels were quantified in decibels (dB) relative to 1.0 g/ms (where 1.0 g = 9.8 m/s^2) and ranged from +6 to −18 dB re: 1.0 g/ms adjusted in 3-dB steps. Electroencephalographic activity was amplified (200,000X), filtered (300 – 3000 Hz), and digitized (100 kHz). Two hundred fifty-six primary responses were averaged and replicated for each VsEP waveform. The first positive and negative response peaks were scored for each VsEP waveform as this initial response peak is generated by the peripheral vestibular nerve. Peak latencies (in milliseconds), peak-to-peak amplitude (in microvolts), and thresholds (in dB re: 1.0 g/ms) were quantified and compared between genotypes using two factor analysis of variance with age and genotype as fixed factors.

2.6 Histology/phenotype evaluation

Fifteen *Kcna10*^{TM45} littermates (3 wild type, 6 heterozygotes and 6 homozygotes) aged between 3.5 to 5 months old were evaluated by the mouse phenotyping core facility at NIH (Office of Research Services Phenotyping Core) for gross and histopathological phenotypes.

2.7 Immunohistochemistry

Rabbit polyclonal antiserum (PB692) was developed to a peptide from the unique N-terminal region of mouse KCNA10 (Fig. 3). This peptide corresponds to amino acid residues 50 to 65 (RVLISDNTNHETAFSK; RefSeq NP_001074609), which is 68% identical to the corresponding region in human KCNA10. Antisera were purified on a Pierce AminoLinkPlus column (#44894, Thermo Scientific), to which we bound the KCNA10 peptide. We also used a commercially available antibody to an epitope from human KCNA10 (Abcam ab28724) that is 96% identical to mouse KCNA10 and corresponds to amino acids 181 to 230. The antisera were validated initially by immunostaining COS7 cells transfected with a vector expressing a GFP-KCNA10 fusion protein.

Wild type and homozygous mutant *Kcna10*^{TM45} mice were sacrificed, and cochleae were harvested according to NIDCD/NIH animal protocol 1263-09. Cochleae were fixed in 4% paraformaldehyde (Electron Microscopy Sciences) for 2 hours, and then washed with PBS. Cochleae were then microdissected to extract sensory epithelia from the organ of Corti and vestibular organs. Tissues were permeabilized with 0.5% Triton-X (Fisher) for 20 minutes and incubated with blocking solution (2% BSA and 5% normal goat serum diluted in PBS)

for 2 hours to prevent non-specific binding. Tissues were incubated with primary antibodies for 2 hours, washed three times with PBS, and incubated with FITC-conjugated anti-rabbit IgG secondary antibody (Molecular Probes) at a 1:400 dilution in blocking solution and rhodamine-conjugated phalloidin at a 1:100 dilution in blocking solution for 20 min. Tissues were further washed with PBS, and then mounted on glass slides using Immu-Mount (Thermo Scientific) and imaged with a Zeiss LSM780 confocal microscope.

3. Results

3.1 RT-PCR of *Kcna10* transcripts in the mouse inner ear

RT-PCR was performed on cDNAs from multiple mouse tissues including adult cochleae (Fig. 1) using a forward primer in exon 1 and a reverse primer in exon 3. Exon 2 is a cassette exon, i.e. the alternate mRNAs transcribed from the *Kcna10* locus differ in either including or excluding exon 2. PCR fragments corresponding to both alternate splice forms of *Kcna10* (with or without exon 2) were consistently detected in adult inner ear in multiple experiments (Fig. 1). The 224 bp amplimer (without exon 2) was also reliably amplified from skeletal muscle, while the 479 bp amplimer (with exon 2) was weakly amplified. Amplimers from both isoforms were also weakly amplified in E15and E17 cDNA. Distinct amplimers were not consistently amplified from cDNA of any other tissues.

3.2 *Kcna10* expression in the mouse inner ear

The single protein-coding exon of *Kcna10* was replaced with an IRES-bGeo/Purocassette which encodes beta–galactosidase, puromycin, and neomycin. The expression of beta–galactosidase under the control of the *Kcna10* promoter and enhancers serves as a proxy for *Kcna10* native expression (Fig. 2). At E18.5 in the organ of Corti, beta-galactosidase expression is observed only in the inner hair cells in a tonotopic gradient, with the strongest expression at the basal turn. This signal gradually diminishes toward the middle turn, after which few individual inner hair cells show beta-galactosidase expression. Additionally, at E18.5, sensory hair cells and supporting cells in utricle, ampullae, and saccule also showed beta-galactosidase activity. At P17, inner hair cells of the entire cochlea exhibit similar levels of beta-galactosidase expression. Some expression was evident in outer hair cells and, to a lesser extent, the supporting cells of the organ of Corti, indicating that *Kcna10* expression in the outer hair cells begins at a time between P1 and P17. Outer hair cell expression is initially strongest at the apical turn of the organ of Corti, and faint expression is discernable at the basal turn. This gradient is present until at least P75. These data indicate that KCNA10 expression develops in the inner and outer hair cells in opposing directions with respect to the base and apex of the cochlea. No detectable beta-galactosidase signal corresponding to KCNA10 expression was observed in other cochlear compartments, including those reported by Carlisle et al (2012) having positive anti-KCNA10 antibody immunoreactivity, such as the stria vascularis, Reissner's membrane, Hensen's cells, Deiters' cells, root cells, Kolliker's organ, interdental cells, marginal cells, and spiral prominence.

We generated an antibody (PB692) to a peptide from the unique N-terminal region of KCNA10 (Fig. 3a). The PB692 antibody co-localizes with a GFP-KCNA10 fusion protein in transfected COS-7 cells (Fig. 3b). Immunolocalization of KCNA10 in the wild type mouse inner ear using PB692 indicated that KCNA10 is present in inner and outer hair cells, as well as internal sulcus cells, border cells, and pillar cells. However, this signal was still present in homozygous *Kcna10* knockout mouse organ of Corti (Fig. 3c). No signal was evident when primary PB692 antibody was omitted, and cochlear tissues were probed with FITC-conjugated anti-rabbit IgG secondary antibody alone. Attempts to immunolocalize with a commercially available antibody (Abcam catalog number ab28724) gave similar

results in homozygous *Kcna10* knockout mice (data not shown). Since the entire protein coding region of *Kcna10* was deleted in the knockout mouse, we concluded that both antisera are multi-specific, and no further immunolocalization analyses were performed.

3.3 Expression of *Kcna10* in other mouse tissues

Multiple organs from the adult $Kcna10^{TM45}$ were examined for beta-galactosidase expression. Brain, heart, lung, and liver from heterozygous and homozygous $Kcna10^{TM45}$ mice did not exhibit any beta-galactosidase expression. Kidney expression could not be evaluated due to endogenous beta-galactosidase-like activity in the wild type kidney (data not shown).

At embryonic day E18.5 we detected expression of beta-galactosidase in the ear. The detailed pattern of expression is shown in the upper panels of Figure 2. At this point, stronger expression of beta-galactosidase was found in the sensory epithelia of all vestibular end-organs while fainter signal was detected in the inner and outer hair cells of the organ of Corti of homozygous (Figure 2) and heterozygous $Kcna10^{TM45}$ but not in wild type control mice. At E18.5, no other tissue exhibited beta-galactosidase expression.

3.4 $Kcna10^{TM45}$ mouse phenotype

The phenotypes of six heterozygous, six homozygous $Kcna10^{TM45}$, and three wild type mice were evaluated for serum chemistries, gross organ morphology, and tissue and cell structure. All wild type mice were males; each of the other two genotype groups consisted of 3 males and 3 females. No significant differences were noted between homozygous mutant $Kcna10^{TM45}$ mice and B6 (wild type) parent strain mice. There was a slight increase in the kidney-to-brain mass ratio for the homozygous mutant but not heterozygous mice when compared to wild type ($p = 0.0276$). However, no differences were observed in the gross or microscopic anatomy in either the brain or the kidney of the $Kcna10^{TM45}$ mouse.

3.5 *Kcna10*-null mice have mildly elevated hearing thresholds

Pure-tone thresholds at each test frequency were compared among genotypes using one-way ANOVA. We detected a statistically significant effect of genotype on response thresholds for 8-kHz and 32-kHz stimuli ($p < 0.05$), with the entire difference attributable to higher thresholds among homozygotes (Fig. 4). However, while statistically significant, these threshold differences are only 5–10 dB, which is generally considered the limit of precision for ABR threshold determination, and so may have no biological significance. No significant threshold differences between wild type and heterozygotes were detected at any frequency.

3.6 *Kcna10*-null mice show severe to profound gravity receptor dysfunction

Kcna10-null mice do not exhibit any circling behavior or overt balance problems, yet vestibular evoked potentials (VsEP) indicate a gravity receptor dysfunction starting as early as P30. VsEP waveforms for homozygous mutants were poorly formed, and have broad response peaks compared to those of heterozygotes (Fig. 5a). P1 was often the only visible response peak and several mutants displayed no VsEPs (3 out of 6 mice at 30 days of age, 3 out of 8 mice at 10 months of age). For those animals where VsEPs could be measured, two-factor analysis of variance was completed for P1 latencies (at +6 dB), P1-N1 amplitudes (at +6dB), and thresholds. A significant main effect of age ($F(1, 18) = 14.03$, $p = 0.001$) was found for P1 latency, but more importantly, a significant main effect of genotype ($F(1,18) = 208.48$, $p < 0.0001$) was identified. P1 latencies in homozygotes were significantly prolonged compared to heterozygotes. At P30, latency differences between homozygotes and heterozygotes averaged 0.3 ms but, by 10 months, the average difference in P1 latency

between genotypes was 1.0 ms (Fig 5c). VsEP thresholds showed a significant interaction between age and genotype ($F(1,19) = 78.73$, $p = 0.0016$) where thresholds were similar at 30 days of age (−3.5 ± 1.5 dB re: 1.0 g/ms for heterozygotes compared to −1.5 ± 3.0 dB for homozygotes), but by 10 months, thresholds were significantly elevated for the knockout mice ($p < 0.001$, −9.0 ± 2.5 dB for heterozygotes compared to −0.9 ± 3.3 dB for homozygotes, Fig. 5b). P1-N1 amplitudes showed a significant main effect for age ($F(1, 18) = 6.65$, $p = 0.01$) where the older animals had significantly larger amplitudes than the younger animals (Fig 5c).

4. Discussion

This study examined the localization and function of KCNA10 in wild type and *Kcna10* knockout auditory and vestibular tissues. Our RT-PCR data suggest that both splice isoforms of *Kcna10* are expressed primarily in the inner ear. This is consistent with our observation of significant abundance from the massively parallel sequencing signatures (MPSS) for *Kcna10* from inner ear libraries. One signature corresponding to exon 3 is abundant in our inner ear libraries but absent from all but one (male amygdala) cDNA library out of the 90 libraries of the Mouse Reference Transcriptome (MRT) database; a second signature corresponding to exon 2 was detected in our inner ear libraries but absent in all but one (female smooth muscle) of the MRT libraries (Peters et al, 2007). It is also notable that all ESTs in the mouse (Mm.245155) and rat (Rn.154486) unigene listings are derived from inner ear cDNA, and there are no spliced ESTs of human *KCNA10* in the unigene assembly (Hs.622910) to provide unambiguous expression data. Our beta-galactosidase expression profile of the $Kcna10^{TM45}$ mouse was consistent with the results from RT-PCR analysis of cDNA from mouse tissues. *Kcna10* expression appears to be limited to the inner ear although we cannot exclude the possibility that *Kcna10* expression is present in kidney due to endogenous beta-galactosidase-like activity in wild-type tissue.

In the inner ear, the beta-galactosidase signal is strongest in the sensory epithelia of the vestibular organs including the utricle, saccule, and ampullae. In the organ of Corti, beta-galactosidase expression begins earlier in the inner hair cells than the outer hair cells, and the onset of expression in the inner hair cells occurs in a base to apex developmental gradient. This follows the developmental pattern of hair cells, where inner hair cells start to differentiate first followed by outer hair cells, and maturation generally occurs in a base to apex gradient (Anniko, 1983). After P12, there is a uniform expression of beta-galactosidase in all inner hair cells. However, beta-galactosidase expression in the outer hair cells is strongest at the apical turn of the organ of Corti as early as P12 (data not shown) and nonexistent in the basal turn. This pattern remains stable until at least P75. The pattern coincides with the functional maturation of OHCs (Lenoir and Puel, 1987). Thus, the beta-galactosidase expression patterns of the IHC and OHC develop in opposite tonotopic gradients.

Our beta-galactosidase reporter expression results as a proxy for *Kcna10* are not consistent with published immunohistochemistry studies of KCNA10 expression. Carlisle et al (2012) used an antibody to an epitope corresponding to amino acids 154 to 203 in human and mouse KCNA10 and observed labelling in many more cell types (Reissner's membrane, neurons, stria vascularis, etc.) than indicated by our beta-galactosidase expression. The epitope targetted by their antibody is 96% identical to mouse KCNA10, but is also 64% identical to mouse KCNA5 and KCNA2. We also attempted to label KCNA10 using a commercially available antibody to the region corresponding to amino acids 181 to 230 as well as our own antibody, PB692, directed to a 16 amino acid peptide derived from the N-terminal region, which shows no similarity to other KCNA proteins in a ClustalW alignment (Fig. 3). Both antibodies labelled structures in the homozygous *Kcna10* knockout mouse,

thus we concluded that neither is specific to KCNA10. The 16-amino-acid epitope used to generate PB692 is 50% identical to a region of CNP (2′,3′-cyclic-nucleotide 3′-phosphodiesterase) encoded by *Cnp*, which is abundant in the inner ear (mouse unigene Mm.15711). This may account for the multi-specificity of our KCNA10 antiserum.

The robust expression of KCNA10 in the vestibular sensory epithelia suggests that it serves an important role in peripheral vestibular function, and the VsEP data confirm a severe to profound gravity receptor deficit in the knockout mice. Overall, the VsEP data suggest that the severe dysfunction in *Kcna10* knockout mice may be related to slowed or dys-synchronous firing of the peripheral vestibular nerve and declining gravity receptor sensitivity with age. Prolonged P1 latencies together with elevated thresholds and poor waveform morphology implicate the hair cell, the hair cell to neuron synapse, or the primary afferent as the source of the functional deficit. A variety of ion channels, including voltage sensitive potassium channels, are known to be responsible for shaping the neural discharge of vestibular primary afferents producing stereotypic phasic and tonic characteristics (Goldberg, 1991; Iwasaki et al, 2008; Eatock et al, 2008; Kelluri et al, 2010; Eatock & Songer, 2011). When potassium channels are disrupted, the timing and pattern of neural discharge can be altered (Iwasaki et al, 2008; Kelluri et al, 2010), which in turn could alter far-field compound action potentials. The characteristics of the compound action potentials recorded here substantiate a hypothesis of altered neural discharge in *Kcna10* knockout mice.

The KCNA10-null mouse does not exhibit any obvious imbalance behaviors such as circling, weaving, or head-bobbing, and swimming behavior that relies on the gravity sensing organs was normal. The lack of an obvious behavioral phenotype has been documented for other mouse strains with significant inner ear gravity receptor deficits (Jones et al, 2005; Goodyear et al, 2012). In the present study, the lack of a behavioral phenotype could be due to sufficient sensory input from the semicircular canals (which were not evaluated) or compensation by the central nervous system. It could also be the case that gravity receptor function is robust at ages younger than P30, contributing to the development of normal motor skills, which are then maintained as the peripheral deficit gradually worsens. The central nervous system has great capacity to compensate for significant inner ear vestibular dysfunction.

In contrast to vestibular function, ABR threshold measurements of KCNA10-null mice showed only slightly elevated thresholds (approximately 5 to 8 dB) in response to 8- and 32-kHz stimuli as compared to those of wild type and heterozygous mice. This suggests KCNA10 plays a minimal role in establishing auditory sensitivity. However, some role for KCNA10 in the cochlea may be suggested by prolonged P1 latencies found for the homozygotes. Furthermore, prolonged P1 latencies would suggest that KCNA10 function is evident at sites similar to those identified above for the vestibular periphery: that is, at the hair cell, the hair cell-afferent synapse, and/or the spiral ganglion neurons. Auditory neurons do not share the neural firing pattern characteristics of vestibular afferents and likely do not share the same complement of ion channels, which may explain the differing results between the auditory and vestibular sensory modalities.

Considering the large number of genes identified for hearing loss, it is noteworthy that no genetic causes for nonsyndromic peripheral vestibulopathies have been identified in humans (Jen, 2011). Although linkage analysis studies have been performed on patients with Menière's disease, no definitive genetic linkage to this disease has been reported (Birgerson et al, 1987; Frykholm et al, 2006; Klockars et al, 2007). The fact that auditory sensitivity remains intact up to 11 months of age in the mouse (data not shown) implies that *Kcna10* plays a more important role in the mouse vestibular periphery than in the cochlea. Therefore,

Kcna10 knockout mouse may prove a useful model for investigators studying the genetics of human vestibulopathies.

Supplementary Material

Refer to Web version on PubMed Central for supplementary material.

Acknowledgments

We thank Drs. Dennis Drayna and Andrew Griffith for their critiques of this study, and Elizabeth Wilson for her assistance in maintaining the *Kcna10*^{TM45} colony. This research was supported by NIH grant R01 DC006443 (S.M.J.) and NIDCD intramural research fund DC000048-15 (T.B.F.)

Abbreviations

P17	postnatal day 17
ABR	auditory brainstem response
VsEP	vestibular evoked potential
ms	millisecond
MIM	Mendelian inheritance in man

References

Anniko M. Postnatal maturation of cochlear sensory hairs in the mouse. Anatomy and Embryology. 1983; 166(3):355–368. [PubMed: 6869851]

Birgerson L, Gustavson K, Stahle J. Familial Menière's disease: a genetic investigation. American Journal of Otology. 1987; 8(4):323–326. [PubMed: 3631240]

Browne D, Gancher S, Nutt J, Brunt E, Smith E, Kramer P, et al. Episodic ataxia/myokymia syndrome is associated with point mutations in the human potassium channel gene, KCNA1. Nature Genetics. 1994; 8(2):136–140. [PubMed: 7842011]

Carlisle F, Steel K, Lewis M. Specific expression of Kcna10, Pxn and Odf2 in the organ of Corti. Gene Expression Patterns. 2012; 12(5–6):172–179. [PubMed: 22446089]

Eatock R, Songer J. Vestibular hair cells and afferents: two channels for head motion signals. Annual Review of Neuroscience. 2011; 34:501–534.

Eatock R, Xue J, Kalluri R. Ion channels in mammalian vestibular afferents may set regularity of firing. Journal of Experimental Biology. 2008; 211:1764–1774. [PubMed: 18490392]

Frykholm C, Larsen H, Dahl N, Klar J, Rask-Andersen H, Friberg U. Familial Ménière's disease in five generations. Otology and Neurotology. 2006; 27(5):681–686. [PubMed: 16868516]

Goldberg J. The vestibular end organs: morphological and physiological diversity of afferents. Current Opinion in Neurobiology. 1991; 1:229–235. [PubMed: 1821186]

Goodyear RJ, Jones SM, Sharifi L, Forge A, Richardson G. Hair-bundle defects and loss of function in the vestibular end organs of mice lacking the receptor-like inositol lipid phosphatase, PTPRQ. Journal of Neuroscience. 2012; 32(8):2762–2772. [PubMed: 22357859]

Gutman G, Chandy K, Grissmer S, Lazdunski M, McKinnon D, Pardo L, et al. International Union of Pharmacology. LIII. Nomenclature and molecular relationships of voltage-gated potassium channels. Pharmacological Reviews. 2005; 57(4):473–508. [PubMed: 16382104]

Iwasaki S, Chihara Y, Komuta Y, Ito K, Sahara Y. Low-voltage-activated potassium channels underlie the regulation of intrinsic firing properties of rat vestibular ganglion cells. Journal of Neurophysiology. 2008; 100(4):2192–2204. [PubMed: 18632889]

Iwasaki S, Nakajima T, Chihara Y, Inoue A, Fujimoto C, Yamasoba T. Developmental changes in the expression of Kv1 potassium channels in rat vestibular ganglion cells. Brain Research. 2012; 1429:29–35. [PubMed: 22079321]

Jen J. Genetics of vestibulopathies. Advances in Oto-rhino-laryngology. 2011; 70:130–134. [PubMed: 21358195]

Jones SM, Johnson KR, Yu H, Erway LC, Alagramam KN, Pollak N, Jones TA. A quantitative survey of gravity receptor function in the mutant mouse strains. Journal of the Association for Research in Otolaryngology. 2005; 6(4):297–310. [PubMed: 16235133]

Jones SM, Robertson NG, Given S, Heisch ABS, Liberman MC, Morton CC. Hearing and vestibular deficits in the Coch null mouse model: Comparison to the CochG88E/G88E mouse and to DFNA9 hearing and balance disorder. Hearing Research. 2011; 272:42–48. [PubMed: 21073934]

Kelluri R, Xue J, Eatock R. Ion channels set spike time regularity in mammalian vestibular afferents neurons. Journal of Neurophysiology. 2010; 104:2034–2051. [PubMed: 20660422]

Kleopa K, Elman L, Lang B, Vincent A, Scherer S. Neuromyotonia and limbic encephalitis sera target mature Shaker-type K+ channels: subunit specificity correlates with clinical manifestations. Brain: a Journal of Neurology. 2006; 129(6):1570–1584. [PubMed: 16613892]

Klockars T, Kentala E. Inheritance of Meniere's disease in the Finnish population. Archives of Otolaryngology -- Head and Neck Surgery. 2007; 133(1):73–77. [PubMed: 17224529]

Kopp-Scheinpflug C, Fuchs K, Lippe W, Tempel B, Rübsamen R. Decreased temporal precision of auditory signaling in Kcna1-null mice: an electrophysiological study in vivo. Journal of Neuroscience. 2003; 23(27):9199–9207. [PubMed: 14534254]

Lang R, Lee G, Liu W, Tian S, Rafi H, Orias M, et al. KCNA10: a novel ion channel functionally related to both voltage-gated potassium and CNG cation channels. American Journal of Physiology. Renal Physiology. 2000; 278:F1013–F1021. [PubMed: 10836990]

Lenoir M, Puel J. Development of 2f1-f2 otoacoustic emissions in the rat. Hearing Research. 1987; 29:265–271. [PubMed: 3624087]

Mathews P, Jercog P, Rinzel J, Scott L, Golding N. Control of submillisecond synaptic timing in binaural coincidence detectors by K(v)1 channels. Nature Neuroscience. 2010; 13(5):601–609.

Peters L, Belyantseva I, Lagziel A, Battey J, Friedman T, Morell R. Signatures from tissue-specific MPSS libraries identify transcripts preferentially expressed in the mouse inner ear. Genomics. 2006; 89(2):197–206. [PubMed: 17049805]

Pongs O. Molecular biology of voltage-dependent potassium channels. Physiological Reviews. 1992; 72:69–88.

Smart S, Lopantsev V, Zhang C, Robbins C, Wang H, Chiu S, et al. Deletion of the K(V)1.1 potassium channel causes epilepsy in mice. Neuron. 1998; 20(4):809–819. [PubMed: 9581771]

The Mouse Transcriptome Project. 2005. Retrieved 2012, from NCBI: http://www.ncbi.nlm.nih.gov/genome/guide/mouse/MouseTranscriptome.html

Tian S, Liu W, Wu Y, Rafi H, Segal A, Desir G. Regulation of the voltage-gated K+ channel KCNA10 by KCNA4B, a novel beta-subunit. American Journal of Physiology. Renal Physiology. 2002; 283(1):F142–F149. [PubMed: 12060596]

Wang H, Kunkel D, Schwartzkroin P, Tempel B. Localizaton of Kv1.1 and Kv1.2, two K channel proteins, to synaptic terminals, somata, and dendrites in the mouse brain. Journal of Neuroscience. 1994; 14:4588–4599. [PubMed: 8046438]

Yao X, Segal A, Welling P, Zhang X, McNicholas C, Engel D, et al. Primary structure and functional expression of a cGMP-gated potassium channel. Proceedings of the National Academy of Sciences of the United States of America. 1995; 92(25):11711–11715. [PubMed: 8524834]

Yao X, Tian S, Chan H, Biemesderfer D, Desir G. Expression of KCNA10, a voltage-gated K channel, in glomerular endothelium and at the apical membrane of the renal proximal tubule. Journal of the American Society of Nephrology. 2002; 13(12):2831–8239. [PubMed: 12444201]

Highlights

- A *Kcna10* knockout mouse was generated to study the role of KCNA10 in the inner ear.
- *Kcna10* is expressed in inner and outer hair cells and vestibular sensory epithelia.
- The *Kcna10* knockout mouse displays mild auditory dysfunction and absent VsEPs.

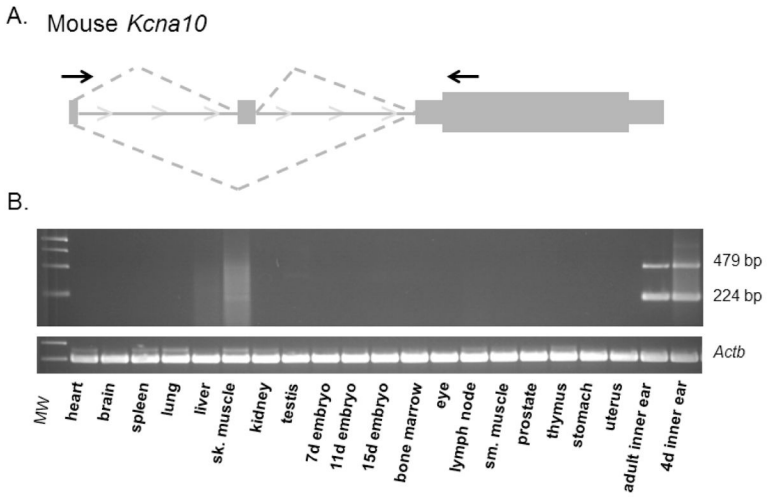

Fig. 1.

(A) Primers (indicated by arrows) in exon 1 and exon 3 were designed to test mouse tissue panels for *Kcna10* mRNA expression. (B) RT-PCR amplification products corresponding to both splice forms of *Kcna10* are detected in the adult inner ear. Expression is also detectable in adult skeletal muscle with the 224-bp product, which lacks exon 2 and is indicated by a single asterisk, more abundant than the 479-bp product (indicated by double asterisks). Faint expression of both isoforms is also evident in E15 and E17cDNA. *Actb* was used as a positive control.

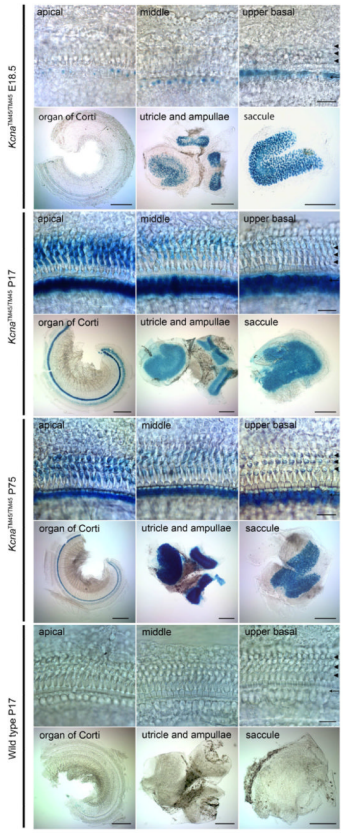

Fig. 2.

Whole-mount X-gal staining of *Kcna10*$^{+/+}$ and *Kcna10*$^{TM45/TM45}$ inner ears. Scale bars in rows 1, 3, 5, and 7 represent 20 μm. Scale bars in rows 2, 4, 6, and 8 represent 200 μm. Inner ears of *Kcna10*$^{TM45/TM45}$ at E18.5 (rows 1 and 2), P17 (rows 3 and 4), P75 (rows 5 and 6), and *Kcna10*$^{+/+}$ P17 (rows 7 and 8) were stained with X-gal for beta-galactosidase activity. At E18.5, outer hair cells show no expression at any turn of the organ of Corti (3 arrowheads). Inner hair cells (single arrow) express beta-galactosidase in a base to apex gradient, with the strongest expression level at the basal turn (top right box), and almost no expression discernible at the apical turn (top left box) of the organ of Corti. Sensory epithelia in the utricle, ampullae, and saccule express beta-galactosidase (row 2). At P17, all inner hair cells show expression. In outer hair cells, expression occurs in a gradient with strongest expression levels of beta-galactosidase in the apical turn (row 3), and faint expression in the basal turn (row 3, column 3). The signal in the sensory epithelia cells in the vestibular organs remains consistent with E18.5 expression (row 4). This expression pattern remains consistent up to P75 (rows 5 and 6). No beta-galactosidase expression is evident in wild type controls (rows 7 and 8).

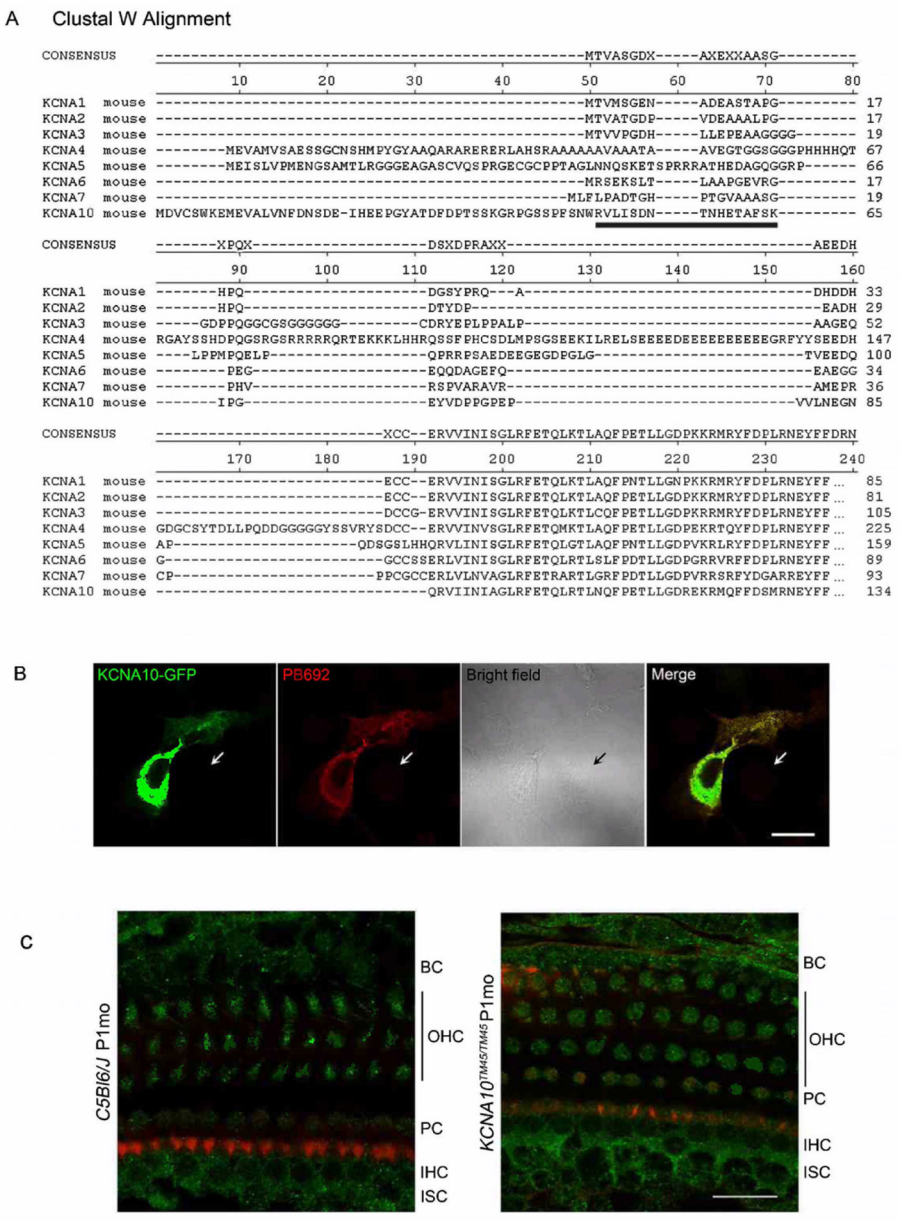

Fig. 3.

The epitope targeted by PB692 (black bar) is unique to KCNA10 amongst the KCNA protein family members as shown in the ClustalW alignment. Consensus was determined by the ClustalW program (http://www.ebi.ac.uk/Tools/msa/clustalw2/). (B) PB692 was validated through a co-localization assay, in which COS7 cells were transfected with KCNA10-GFP (green) and stained with PB692 (red). Nontransfected cells (arrows) did not express KCNA10-GFP, nor exhibit any signal from PB692. Scale bar represents 20 μm. (C) Immunostaining of wild type P20 organ of Corti shows PB692 signal (green) in multiple cell types, including inner hair cells (IHC) and outer hair cells (OHC), border cells (BC), internal sulcus cells (ISC), and pillar cells (PC) (left panel). However, this signal persisted in *Kcna10*$^{TM45/TM45}$ tissues (right panel), indicating that PB692 is non-specific. Rhodamine phalloidin (red) was used to stain actin. Scale bar represents 20 μm.

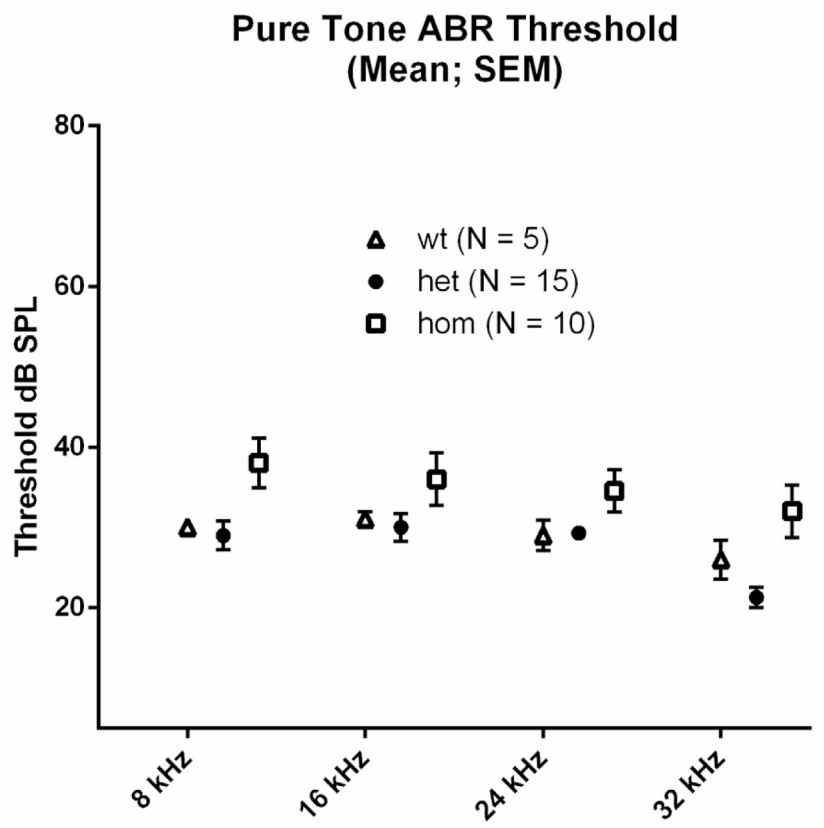

Fig. 4.

Pure-tone ABR thresholds were mildly elevated in homozygotes when compared to their heterozygote and wild type littermates at 8 kHz ($P<0.05$*) and 32 kHz ($P<0.01$**). There were no significant differences in thresholds between heterozygotes and wild type littermates at any frequency. All animals were tested at approximately 3 months age.

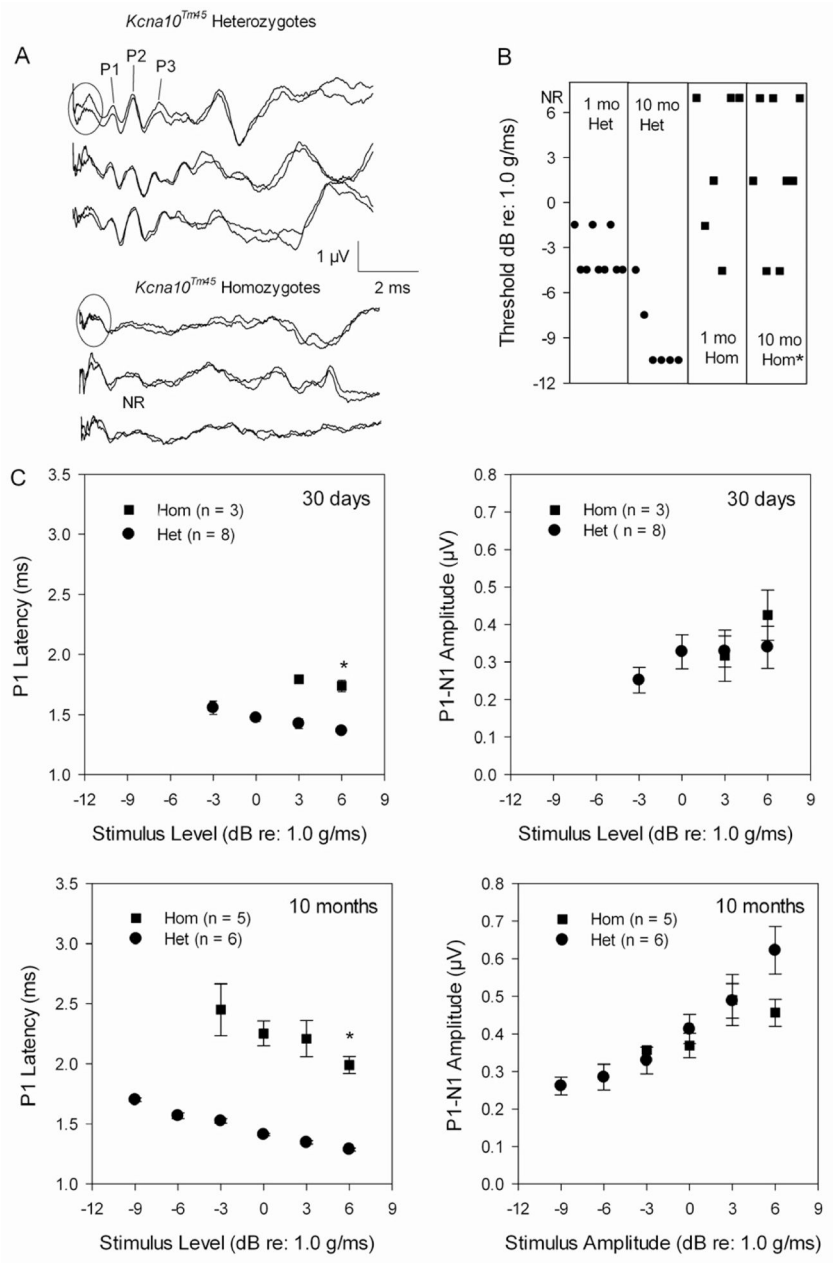

Fig. 5.

(A) VsEPs collected at +6 dB re: 1.0g/ms for three 10-month-old *Kcna10*^{Tm45} heterozygotes showed normal waveform morphology while age-matched homozygotes displayed waveforms with poor morphology and only a broad-shaped P1 visible. The initial portion of each waveform (circled region) represents masker artifact since the VsEPs were collected during the presentation of a broadband forward masker (94 dB SPL, 20- to 50-kHz) to eliminate auditory responses. (B) In addition to poor waveform morphology, *Kcna10*^{Tm45} homozygotes had significantly elevated thresholds at 10 months of age. At 30 days of age, 3 homozygotes had absent VsEPs. (C) At both ages, *Kcna10*^{Tm45} homozygotes showed significantly prolonged P1 latencies compared to heterozygotes. On average, P1-N1 amplitudes were similar for the two genotypes. The asterisks identify statistically significant findings.